THE JOURNAL OF PHYSICAL CHEMISTRY A

 VOLUME 112, NUMBER 35, SEPTEMBER 4, 2008

ARTICLES

Ion-Pairing of Octyl Viologen Diiodide in Low-Polar Solvents: An Experimental and Computational Study

Giacomo Saielli*

Istituto per la Tecnologia delle Membrane del CNR, Sezione di Padova, Via Marzolo, 1-35131 Padova, Italy

Received: March 31, 2008; Revised Manuscript Received: June 24, 2008

We have investigated the ion-pairing and solvent effect on the NMR and UV/vis spectra of 1,1′-di-*n*-octyl-4,4′-bipyridinium diiodide in various solvents. A strikingly different behavior is observed in the low polar solvent dichloromethane. A large deshielding of the *meta* bipyridinium core resonance occurs and charge transfer (CT) transitions are observed in the visible region due to the formation of ion-pairs. The CT bands show a marked blue-shift as the polarity of the solvent is increased. Experimental data have been compared with the results of DFT calculations of proton's chemical shifts and TD-DFT calculations of the vertical electronic transitions of model ion-pairs (using the smaller methyl viologen dication) in the gas phase and after the inclusion of the solvent reaction field by means of the PCM scheme. Different geometrical arrangements of the ion-pairs have been investigated, and the direct and indirect solvent effect has been elucidated. A good agreement is obtained which allows one to get insights concerning the CT transitions of this system and the geometry of the ion-pairs in solution of low-polar solvents.

Introduction

1,1′-Dialkyl-4,4′-bipyridinium salts, also known as viologens, have received a great deal of attention because of their many interesting properties: they can exist in three different redox forms, the dication, the stable, and intensely colored, radical monocation and the fully reduced neutral form;[1] they can be used, with appropriate catalysts, to photochemically produce hydrogen from water;[2] their redox properties render viologens, particularly the lowest homologue of the series, methyl viologen, rather toxic. The dichloride salt of methyl viologen is commercially known as Paraquat, and it is a potent herbicide.[1] They have been employed as chemosensors for the detection of glucose,[3] dopamine[4] and NADP,[5] in electrochromic devices[6] and to induce a shuttle motion in molecular devices.[7]

Recently, 1,1′-dialkyl-4,4′-bipyridinium salts having relatively long alkyl chains have been the subject of some investigations because of their liquid crystalline properties.[8] It appears that the counteranion is essential to induce the liquid crystalline state, usually a smectic A phase. Bromide and iodide salts of di-*n*-heptyl and di-*n*-octyl bipyridinium do not show any mesomorphic behavior. However, once the halide anion is replaced with the more bulky and less symmetric *bis*(trifluoromethane)sulfonimide (Tf_2N) a stable room temperature smectic A phase appears.[9]

Despite the renewed interest in viologen salts with relatively long alkyl chains, no systematic investigation of the solvent and ion-pairing effects on their spectroscopic properties has yet appeared, particularly concerning the intermolecular charge transfer (CT) band between a suitable anion and the dication.[1] The ion-pairing process and the structure and stoichiometry of the ion pairs in low and nonpolar solvents are of importance

* Fax: +39-049-8275239. E-mail: giacomo.saielli@unipd.it.

10.1021/jp802747h CCC: $40.75
Published on Web 08/01/2008

especially in view of the use of viologen salts as guests in inclusion complexes.[10] In these cases the host−guest equilibrium is strongly affected by the ion-pairing equilibrium.[11]

Similarly, DFT calculations of their spectroscopic properties are rather scarce: recently Di Matteo reported an extensive computational study of the vibrational, electronic and magnetic properties of methyl viologen dication, MV^{2+}, in its three redox states, in gas phase and in water.[12] Current TD-DFT methods are capable of predicting vertical electronic transitions with relatively high accuracy.[13,14] Of course, such accuracy can only be achieved once the geometry of the system is well-known and, again, for covalent molecules DFT methods are perfectly up to the task.[13a] Long-range solvent effects can also be effectively taken into account by continuum models like PCM.[15] However, intermolecular charge transfer (CT) transitions are known to be poorly described by standard TD-DFT approaches, especially if using pure functionals[16] although significant improvements can be obtained by using long-range corrected functionals.[17,18] Such failure is particularly dramatic when there is a vanishing orbital overlap between the donor and the acceptor moieties. Indeed, a few recent reports have shown that when this is not the case, also standard hybrid functionals, which partly incorporate the correct Hartree−Fock exchange, may provide valuable insights for systems where CT transitions occur.[19−21] For example, CT absorption bands for an ion pair in water have been calculated at the TD-B3LYP level for model geometries, resulting in excellent agreement with the experiments.[22]

Another serious issue arises when treating noncovalent systems, like ion-pairs in solution. In these cases the weak link of any computational protocol is in obtaining the correct geometry. Indeed, there might not be a unique geometry for an ion-pair in solution. A proper investigation would require a full molecular dynamics simulation to generate a number of equilibrium configurations to be used as input for the QM calculations of the desired property. As an example, we have recently reported applications of such computational protocol to the prediction of spectroscopic properties (NMR) of glucose in water[23] and pure ionic liquids.[24] In those cases the MD simulations were capable of sampling the configuration space of the system, either because the system was composed by a single glucose molecule in water and the average was calculated over a relatively long simulation time of 10 ns, sampling every 100 ps, for a total of 100 points; or because it was composed only by a collection of "ion-pairs" (that is without the solvent), of the order of $\sim 10^2$ molecules, and the average was calculated over the final equilibrium configuration, thus for a similar number of points as in the previous case.

In contrast, the case of an ion-pair in solution poses additional severe limitations: to correctly sample the entire configuration space of an ion-pair in solution, which would be, most of the time, present as separate ions, a simulation box containing a large number of ion-pairs at the correct concentration, let us say of the order of $\sim 10^2$ ion-pairs (plus the solvent!), or a very long simulation, would be required. This would make the computational protocol impractical, particularly considering the subsequent QM calculations required.

In this work we report on the solvent and ion-pairing effects on the NMR and UV/vis spectra of 1,1′-di-*n*-octyl-4,4′-bipyridinuim diiodide, octyl viologen (OV) iodide hereafter. The experimental data have been compared with DFT calculations of viologen's chemical shifts and TD-DFT calculations of vertical electronic transitions: several model systems with different geometrical arrangement have been considered; calculations were run in the gas phase and with the inclusion of the solvent reaction field (PCM). For comparison purposes the NMR and UV/vis spectra of octyl viologen dibromide have also been acquired.

The comparison of the calculated and experimental spectra gives useful insights on the structure of the ion-pairs in solution. The good agreement obtained also allows a charaterization of the electronic transitions and assignment of the CT bands observed in the visible region of the spectrum.

Experimental Section

DFT Calculations. Geometries were optimized at the B3LYP/6-311G** level of theory.[25] All minimized geometries were checked by frequency calculations to be true minima. Frequency calculations also provided the relevant thermodynamic quantities at 298 K. Optical transitions (singlet vertical electronic transitions) were calculated with the PBE0 functional, which proved to be very effective in the calculation of excitation energies even for relatively high excited states.[13] Recent tests on the performance of various functionals in TD-DFT calculation of the UV/vis spectrum of several organic dyes (excluding cases of intermolecular charge transfer transitions) showed that PBE0 results have a mean absolute error of just 0.14 eV.[14] For intermolecular CT transitions, provided that orbital overlap is nonvanishing, semiquantitiative results can be obtained with the PBE0 functional, which may provide useful insights on the optical spectra of complex sytems.[19] However, for comparison purposes, vertical electronic transitions at the MP2/SOPPA and CCSD/SOPPA level,[26] using the software package Dalton,[27] have been calculated for the small model system pyridinium bromide and compared with TD-DFT results. Basis sets of Dunning were used in this case.[28] Ab initio results, probably not converged with respect to the basis set, differ from TD-DFT results (which are, instead, converged with respect to the basis set) by about 0.4 eV and, as found in ref 19, the energy of TD-DFT transitions is underestimated compared to the ab initio results. These data are collected in Supporting Information, Figure S9.

For the remaining calculations on the ion-pair model systems of the viologen investigated, 6-31++G** basis set was used for light atoms[29] and the 6-311G** basis set was used for I.[30] Diffuse functions are important particularly for the calculation of high energy transitions in relatively small molecules.[31] To check whether this was necessary for iodide here, a test with the aug-cc-pVDZ-PP[28] was done not showing significant qualitative differences in the calculated spectra, see Figure S7 in Supporting Information; similarly, a second test with the basis set LANL2DZdp for iodide,[32] having relativistic effective core potentials for the core electrons, gave almost identical results to the 6-311G** (Figure S8). For the NMR calculations, we used the B3LYP functional together with the cc-pVTZ basis set for the light atoms[28] and again the 6-311G** basis for iodide. This level of theory has been thoroughly tested.[33] In this case the effect of the basis set of iodide is expected to play a very small role in the NMR properties of the viologen dication. Calculated shielding constants of the reference compounds (^{1}H and ^{13}C in TMS and ^{14}N in CH_3NO_2) were 31.617 ppm, 183.63 ppm and −155.18 ppm, respectively, at the same level of theory. Calculated values are averages of chemically equivalent protons. When considering the solvent reaction field we used the PCM model.[15] All calculations were run using the Gaussian03 software package.[34] Basis sets were downloaded from Basis Set Exchange Web site.[35] The simulated UV/vis spectra were obtained as a sum of Gaussian functions with a width of 3000 cm^{-1} centered at the calculated transition energy.[36]

SCHEME 1: Structural Formula of 1, 1,1′-Di-*n*-octyl-4,4′-bipyridinium Salts, X = Br, I

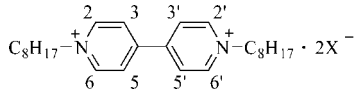

1

NMR and UV/Vis Spectroscopy. ^{1}H, ^{13}C and ^{14}N spectra have been recorded at 400, 100 and 29 MHz, respectively, with a 5 mm multinuclear BBI probe-head, in deuterated dichloromethane, methanol and water. Proton chemical shifts were referred to TMS through the solvent residual signal at 5.32, 3.31 and 4.79 ppm, for CD_2Cl_2, CD_3OD and D_2O, respectively;[37] carbon and nitrogen chemical shift scales were referred to TMS and CH_3NO_2, respectively, through the lock signal.

UV/vis spectra have been recorded using a Perkin-Elmer Lambda 16 spectrophotometer and quartz couvettes with 1 cm and 1 mm optical path. Solvents were of HPLC grade and used without further purification.

1,1′-Di-*n*-octyl-4,4′-bipyridinium Diiodide (OVI_2). 500 mg (3.20 mmol) of 4,4′-bipyridine was added to a mixture of 1.8 mL of iodooctane and 7 mL of acetonitrile and refluxed for 24 h. The red precipitate was filtered and washed with cold acetone (0 °C) and then recrystallized from a mixture of water/acetone 15:85 v/v. Yield: 80%. ^{1}H NMR (400 MHz, CD_3OD): δ = 9.32 (d, $^3J_{HH}$ 6.5 Hz, 4 H, H2, H6, H2′, H6′), 8.71 (d, $^3J_{HH}$ 6.5 Hz, 4 H, H3, H5, H3′, H5′), 4.78 (t, $^3J_{HH}$ 7.6 Hz, 4 H, N−CH_2−R), 2.12 (m, 4H, N−CH_2−CH_2−R), ∼1.44 (m, 20 H), 0.91 (m, 6 H, R−CH_3) ppm. ^{13}C NMR (100 MHz, CD_3OD): δ = 150.3 (C4, C4′), 146.1 (C3, C5), 127.3 (C2, C6), 62.3 (N−CH_2−R), 31.9, 31.6 (N−CH_2−CH_2−R), 29.2, 29.1, 26.3, 22.7, 13.4 (R−CH_3) ppm. ^{14}N NMR (28.9 MHz, CD_3OD): −164.2 ppm. ESI-MS: m/z = 191 [M^{2+}], 269 [M − C_8H_{17}]$^+$. Elemental analysis: found C 49.10%, H 6.72%, N 4.42%; calcd C 49.07%, H 6.65%, N 4.40%.

1,1′-Di-*n*-octyl-4,4′-bipyridinium Dibromide ($OVBr_2$). 500 mg (3.20 mmol) of 4,4′-bipyridine was added to a mixture of 1.5 mL of bromooctane and 6 mL of acetonitrile and refluxed for 24 h. The yellow precipitate was filtered and washed with cold acetone (0 °C) and then recrystallized from water/acetone 15:85 v/v. Yield: 80%. ^{1}H NMR (400 MHz, CD_3OD): δ = 9.32 (d, $^3J_{HH}$ 6.5 Hz, 4 H, H2′, H6′), 8.71 (d, $^3J_{HH}$ 6.5 Hz, 4 H, H3′, H5′), 4.78 (t, $^3J_{HH}$ 7.6 Hz, 4 H, N−CH_2−R), 2.12 (m, 4H, N−CH_2−CH_2−R), ∼1.44 (m, 20 H), 0.91 (m, 6 H, R−CH_3) ppm. ^{13}C NMR (100 MHz, CD_3OD): δ = 150.3 (C4, C4′), 146.1 (C3, C5), 127.3 (C2, C6), 62.3 (N−CH_2−R), 31.9, 31.6 (N−CH_2−CH_2−R), 29.2, 29.1, 26.3, 22.7, 13.4 (R−CH_3) ppm. ^{14}N NMR (28.9 MHz,CD_3OD): −164.2 ppm. ESI-MS: m/z = 191 [M^{2+}], 269 [M − C_8H_{17}]$^+$. Elemental analysis: found C 57.57%, H 7.97%, N 5.22%; calcd C 57.57%, H 7.80%, N 5.16%.

Results and Discussion

1,1′-Di-*n*-octyl-4,4′-bipyridinium, diiodide (and dibromide), **1**, see Scheme 1, were prepared following synthetic protocols reported in the literature,[8] by refluxing the desired amount of bipyridine with an excess of the appropriate halooctane. The octyl viologen iodide crystals are deep red while the analogous bromide crystals are pale yellow.

The color of the salts is due to a charge transfer transition in the solid state between anion and cation:[1] therefore the iodide salt has a strong and low energy charge transfer absorption while the bromide salt has a higher energy charge transfer absorption.

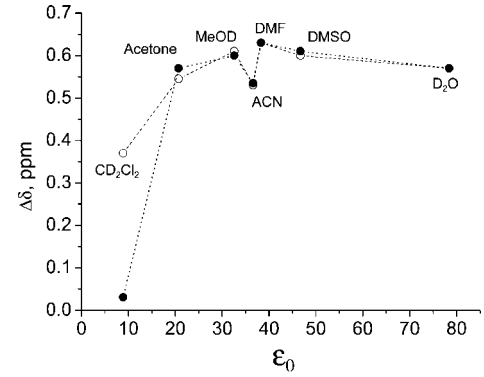

Figure 1. Relative chemical shift, $\Delta\delta = \delta(H_o) - \delta(H_m)$ (H_o = *ortho* protons, H_m = *meta* protons of the bipyridinium core) of OVI_2 (solid circles) and $OVBr_2$ (empty circles) in several solvents of different polarity.

An important issue connected with the intensity of the CT absorption band is the structure of the dication, particularly concerning the dihedral angle between the two pyridine rings. As a general rule it has been found that the CT band is strong when the structure is planar. Indeed, the X-ray structure of the isomorphous methyl viologen bromide and iodide features a planar bipyridinium dication with the halide anions positioned about perpendicular to the C(*ortho*)−N bond.[38] A similar geometrical arrangement is also observed in the X-ray structure of the diethylviologen iodide.[39]

It is known that viologen salts, especially in low polar solvents, undergo a self-association process leading to the formation of ion-pairs, as shown in eq 1 (OV^{2+} octyl viologen dication, X halide anion).[1]

$$OV^{2+} + nX^- = OVX_n^{(2-n)+} \quad K_{eq} = [OVX_n^{(2-n)+}]/[OV^{2+}][X]^n \quad (1)$$

Diluted water solutions are noncolored, while methanol solutions appear yellow-orange for the iodide salt and dichloromethane solutions appear yellow for the dibromide salt and red for the iodide salt. This indicates that some aggregation occurs in low-polar solvents giving rise to the intermolecular charge-transfer bands also observed in the solid state. Also, a marked solvent effect is observed for the octyl viologen iodide salt.

As reported for analogous systems,[10] we did not find any evidence of large aggregates in solution. The very different solubility of OVI_2 in various solvents of different polarity (up to several mg/mL in methanol, less than 0.1 mg/mL in dichloromethane, while it is not soluble in chloroform and benzene[40]) suggests that the value of n in eq 1 should be limited to small values, likely n = 1, 2. Ion-pairing, in dichloromethane, of octyl viologen with tosylate and hexafluorophosphate was studied in ref 10b, and a strong dependence was observed on the counteranions: tight ion pairs were formed with tosylate, while the interaction with PF_6^- seemed to be much weaker.

NMR Spectroscopy and DFT Calculation. In Figure 1 we show the relative chemical shift, $\delta(H_o) - \delta(H_m)$ (H_o = *ortho* protons, that is H-2, H-2′, H-6, H-6′, H_m = *meta* protons, that is H-3, H-3′, H-5, H-5′) in several solvents. In all cases, except dichloromethane, the relative position is essentially constant. Also, no difference can be found between the iodide and bromide salt. In contrast, in dichloromethane, the two resonances are almost overlapped for the iodide salt and they differ from the values obtained for the bromide salt.

TABLE 1: Experimental Chemical Shifts (ppm) of the Aromatic Protons of the OV^{2+} Dication

		$\delta(^1H_o)$	$\delta(^1H_m)$	$\Delta\delta$
OVI_2	D_2O	9.12	8.55	0.57
	CD_3OD	9.32	8.71	0.61
	CD_2Cl_2	9.23	9.20	0.03
$OVBr_2$	D_2O	9.13	8.55	0.58
	CD_3OD[a]	9.33	8.72	0.61
	CD_3OD	9.29	8.69	0.60
	CD_2Cl_2	9.55	9.18	0.37

[a] Concentrated solution, 60 mg/mL.

A more detailed analysis can be done for the three selected solvents, water, methanol and dichloromethane, see Table 1 and Figure 2. In dichloromethane the chemical shift is quite different from the corresponding values in the polar solvents and marked differences are observed between the iodide and the bromide salt. This clearly indicates that ion-pairing processes occur in the low-polar solvent and that they are particularly effective for OVI_2: the formation of ion-pairs produces a large deshielding of the *meta* resonance (from about 8.5−8.7 ppm in polar solvents to 9.2 ppm) while the *ortho* resonance is much less affected. As a result the two signals, of OVI_2 in CD_2Cl_2, are almost overlapped (assignment has been confirmed by an HMQC experiment, see Figure S4 in Supporting Information).

Since the iodide salt shows the most evident solvent and ion-pairing effects, we have considered ion-pair model systems made of methyl viologen (MV^{2+}) dication with iodide. The alkyl chains certainly contribute to the thermodynamics of the association process, but they are likely to play almost no role in the spectroscopic properties of the bipyridinium core while their inclusion would largely complicate the conformational analysis. Calculation of the NMR properties of the model ion pairs are expected to give insights in the geometry of the anions with respect to the viologen dications and to explain, at least qualitatively, the large deshielding of the *meta* resonance.

Model systems were minimized in gas-phase (MVI^+ models A and B and MVI_2 models C and D) or using the solvent reaction field of dichloromethane (MVI^+ models A′, B′). Models A and A′ and C are obtained from the X-ray structure of methyl viologen iodide;[38] the optimized geometries feature the halide anion on top of the *ortho* position of a pyridine ring, slightly shifted outside the ring, an arrangement similar to the crystal structure. We have also considered a different arrangement compared to the crystal structure, models B and B′ and D, where the anion is close to the two *para* carbon atoms. In fact, based on the observed ^{13}C NMR resonances (see Figure S2 in Supporting Information) C-4 and C-4′ are also expected to be positively charged.

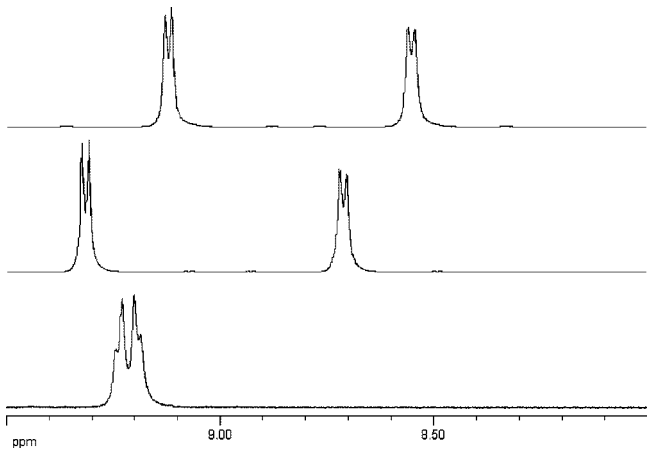

Figure 2. ^1H NMR spectra of OVI_2 (aromatic region) in (top) D_2O, (medium) CD_3OD and (bottom) CD_2Cl_2.

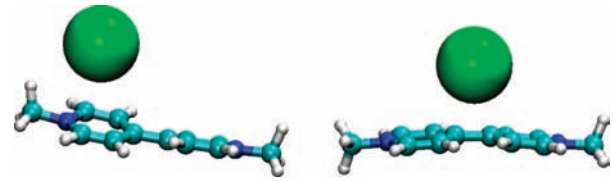

Figure 3. Gas-phase optimized structures (left, model A; right, model B) of MVI^+ ion-pair.

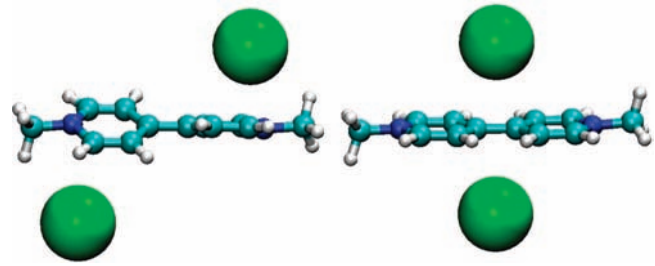

Figure 4. Gas-phase optimized structures (left, model C; right, model D) of MVI_2 ion-pair.

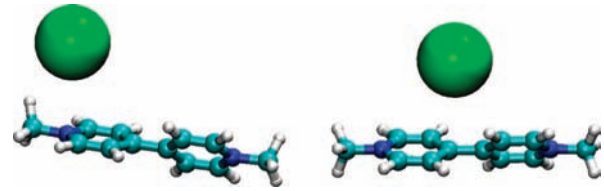

Figure 5. Solution-phase (CH_2Cl_2) optimized structures (left, model A′; right, model B′) of MVI^+ ion-pair.

TABLE 2: Some Geometrical Parameters of the Methyl Viologen Ion-Pairs, MVI^+ and MVI_2, Investigated

model	SCRF	R (Å)[a]	ϕ (deg)[b]
A	gas	2.884	21.2
A′	CH_2Cl_2	3.659	39.6
B	gas	3.016	4.1
B′	CH_2Cl_2	3.874	40.2
C	gas	3.010	28.4
D	gas	3.298	0.1
X-ray[c]		3.840	0.0

[a] Distance, R, between the halide anion and the closest carbon atom of the cation. [b] Dihedral angle ϕ between the two pyridine rings. [c] Reference 38.

Optimized geometries are reported in Figures 3, 4 and 5 while some geometrical parameters are collected in Table 2. It is noteworthy that the gas-phase optimized structures of models B and D feature an almost planar bipyridinium ring together with a short bipyridinium-halide separation.

Inclusion of long-range solvent effects in the optimization increases the separation between the ions. At the same time, the coplanarity of the two rings is reduced since the larger separation implies a less efficient charge-transfer in the ground-state of the ion-pair. We remark here that the optimized structures only represent tentative guesses of the most likely ion-pair structure in solution rather than true static geometries. Indeed, we expect a rather broad distribution of the probability of the anion's relative position with respect to the bipyridinium core, whose density profile, as mentioned in the Introduction, could be obtained only after very expensive molecular dynamics simulation.

TABLE 3: Calculated $\delta(^1H)$ of the Aromatic Protons (ppm) of MV^{2+} and of the Ion-Pair Models Investigated

		$\delta(^1H_o)$	$\delta(^1H_m)$	$\Delta\delta$
MV^{2+}	gas	8.93	8.33	0.60
	CH_2Cl_2	9.14	8.70	0.44
MVI^+ A	gas	8.00	7.71	0.29
	CH_2Cl_2	8.76	8.50	0.26
MVI^+ A′	CH_2Cl_2	9.11	8.61	0.50
MVI^+ B	gas	7.65	7.85	−0.20
	CH_2Cl_2	8.41	8.57	−0.16
MVI^+ B′	CH_2Cl_2	8.98	8.76	0.22
MVI_2 C	gas	9.02	8.13	0.89
MVI_2 D	gas	8.25	8.80	−0.55

It is, however, useful to estimate the complexation free energy of the various models. To this end we have evaluated the entropy contribution from the thermochemistry results (see Experimental Section) in the gas phase; $T\Delta S$ amounts to −5.2, −5.4, −9.6 and −11.2 kcal/mol for models A and B (MVI^+) and C and D (MVI_2), respectively. The energy contribution is evaluated including the solvent reaction field of dichloromethane; it is then calculated as a difference of the PCM/SCF energies before and after complexation and amounts to −4.0, −0.9, −10.5 and −4.0 kcal/mol for model A and B (MVI^+) and C and D (MVI_2), respectively. Thus the estimated complexation free energies are +1.2, +4.6, −0.9 and +7.2 kcal/mol for the four models. From these results it appears that model D, qualitatively corresponding to the arrangement found in the crystal structure, is the most stable. However, due to the complexity of the system treated, the neglect of the dynamical effects and inherent approximations of DFT protocols, mainly the inaccurate treatment of dispersive interactions,[41] the differences in free energy do not allow one to discard or select unambiguously a particular model geometry. The relatively small values of ΔG obtained also confirm that the ion-pairing equilibrium (eq 1) of octyl viologen diiodide in dichloromethane is not quantitatively shifted to the left. 1:1 and 1:2 stoichiometry, therefore, with some amount of free iodide anion, coexist in solution. For comparison, when the free energies of the model geometries A−D were calculated using the solvent reaction field of benzene we obtain −49.6, −47.2, −79.8 and −68.7, respectively, clearly indicating that only neutral ion-pairs would be formed in this nonpolar solvent.

Additional insights can be obtained by calculating the NMR parameters of the various model systems. Thus we have calculated, with DFT methods, see Experimental Section, the proton chemical shifts of the methyl viologen dication and of the model ion-pairs. Results are collected in Table 3.

For the isolated MV^{2+} dication, the chemical shift difference between *ortho* and *meta* resonance is correctly reproduced, in magnitude and sign, and also the calculated chemical shifts are in rather good agreement with the experimental values obtained in polar solvents, where, presumably, no significant ion-pairing occurs. The effect of the iodide anion(s) on the aromatic chemical shifts is to deshield the closer protons; such deshielding effect was already observed for ion-pair model systems of ionic liquids based on the 1-butyl-3-methylimidazolium ([bmim]) cation with BF_4^-, $MeSO_4^-$, PF_6^- and Tf_2N^- anions.[24] Thus models B and D predict an order of the *ortho* and *meta* resonances reversed, compared to the experiments, while the other models still predict the *ortho* resonances to be more deshielded than the *meta* resonances. This is particularly evident for model D, correponding to the X-ray structure. Recalling that the experimentally observed chemical shift is an average of the signals of the various species in eq 1, models B and D are the only ones that can account for the large deshielding of the *meta* resonances observed in dichloromethane.

Concerning carbon and nitrogen chemical shifts, there are no large variations in the three solvents investigated, although in dichloromethane the *meta* carbon resonance is deshielded and the relative separation is reduced, compared to the polar solvents, similarly to the proton resonances. Unfortunately the low solubility in CD_2Cl_2 did not allow the acquisition of a ^{14}N spectra in this latter solvent. Experimental and calculated carbon and nitrogen chemical shifts are reported in Tables S4 and S5 of Supporting Information.

It is somewhat surprising that solvent and counteranion effects are relatively small in the ^{13}C and ^{14}N NMR spectra. Nevertheless, the same behavior was found in the aromatic signals (^1H, ^{13}C and ^{14}N) of the analogous [bmim] cation in pure ionic liquids by varying the counteranion.[24,42] While ring proton resonances of [bmim] were strongly influenced by the counteranion, therefore by changes in the environment, carbon and nitrogen were very little affected, not showing a clear, systematic trend as a function of the counteranion. This apparently puzzling result, especially concerning the large solvent effects usually found in nitrogen shieldings,[43] may be explained recalling that the strong positive charge delocalized on the bipyridinium ring, as well as on the imidazolium ring of [bmim] based ionic liquids, renders the aromatic core almost insensitive to polarization effects induced by the environment.

The preliminary conclusion that can be drawn from the NMR data analysis is that the probability distribution of the iodide anions should have a significant density also close to the C-4 and C-4′ positions, in contrast to the structure which is found in the crystal phase. This may be partly explained also by the presence of a relatively long alkyl chain close to the *ortho* positions. In the liquid phase the many possibilities of gauche conformations of the C−C bonds make it likely for the chain to recoil reducing the space available for the anions.

UV/Vis Spectroscopy. Solutions of OVX_2 have been prepared, in the range of concentrations 10^{-5}−10^{-3} M, in water, methanol, acetone and dichloromethane. We expect the dication, OV^{2+}, to have a typical absorption band in the UV region, connected with a HOMO−LUMO transition involving the π orbitals of the bipyridinium core, similarly to the analogous methyl viologen dication.[12] In contrast, the ion-pairs may show a charge-transfer band, depending on the chemical nature of the anion, which behaves as a charge donor, while the bipyridinium core is the acceptor. Clearly the extinction coefficient of the CT band depends on the analytical concentration of salt since this affects, through the equilibrium constant of eq 1, the concentration of the ion-pairs in solution. In the following we report the extinction coefficients calculated with respect to the analytical concentration of salt, but it should be remembered that the effective concentration of ion-pairs in solution is not known. Methods to determine the equilibrium constants are available,[44] but such study is beyond the scope of the present investigation. We may expect an increase of the apparent extinction coefficient as we move from polar to low-polar solvents since the equilibrium of eq 1 will be shifted to the right as the polarity of the solvent is decreased. Nevertheless, we are concerned with the position of the absorption bands, which is not affected by the concentration, except for a few nm's shift for very diluted solutions. Therefore this aspect has been neglected here. More important, as we move to less polar solvents we expect the CT band to be shifted to longer wavelengths. This red-shift will be the result of a stronger destabilization of the ground state compared to the excited state. In fact, in the excited state the charge separation of the ion-pair is reduced, compared to the ground state, since a fraction of

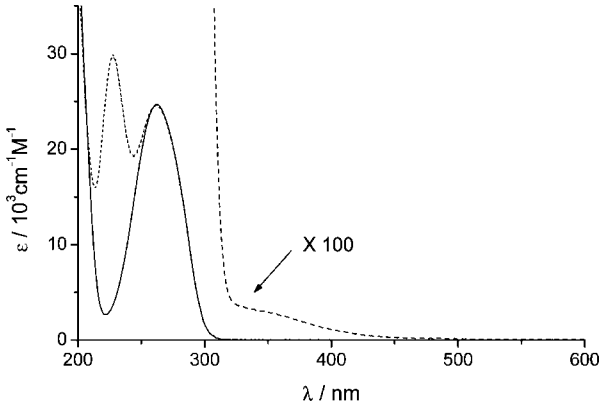

Figure 6. UV/vis spectra, in water at 30 °C, of (solid line) $OVBr_2$ 1.44×10^{-4} M, (dot line) OVI_2 3.80×10^{-4} M, and (dash line) OVI_2 1.5×10^{-3} M.

TABLE 4: Experimental λ_{max} (nm) of the Main Absorption Bands of the Various Systems Investigated

	H_2O	MeOH	acetone[a]	CH_2Cl_2
OVI_2	262	265	–	270
				~320
	~350	379	482	506
$OVBr_2$	262	265		270
				388

[a] The UV absorption of the solvent is overlapped with the bipyridinium core transition.

electron is delocalized from the anion to the bipyridinium system. This is in contrast to the more common cases of charge transfer systems, like push−pull molecules, where the excited state has a higher charge separation than the ground state. There, a red-shift is observed as the solvent polarity is increased.[45]

In Figure 6 we show the UV/vis spectra of OVX_2 (X = Br, I) in water. The typical UV absorption band of the dication appears at 262 nm, with an extinction coefficient of 24600 M^{-1} cm^{-1}. For comparison methyl viologen has maximum absorption at 257 nm with an extinction coefficient of 20700 M^{-1} cm^{-1}.[46] The UV band of the dication is red-shifted as the polarity is decreased, to 265 nm in methanol and to 270 nm in dichloromethane, see Table 4. For high concentrations of OVI_2 in water we also observe a weak absorption band at about 350 nm that may be attributed to the charge transfer between the iodide and the dication. For solutions of methyl viologen iodide in water at 298 K an analogous band was observed at 387 nm with an extinction coefficient of 184.4.[47]

The intense absorption at 227 nm is due to the iodide anion and will not be discussed here.[48] We just recall that the iodide anion, in the gas phase, does not have bound electronic excited states.[48b] The intense UV absorption observed in solution has been attributed to CTTS (charge-transfer-to-solvent) states, and it cannot be modeled without considering explicitly the surrounding cage of solvent molecules.

The CT band of the octyl viologen iodide system is much more evident in less polar solvents. UV/vis spectra are shown in Figure 7. As expected the apparent extinction coefficient is largely increased in dichloromethane compared to methanol and the maximum of the absorption band is shifted to the red as we decrease the medium polarity. It is noteworthy that in dichloromethane a third absorption band is evident, besides the UV absorption of the dication (not shown in Figure 7) and the low energy CT transition; such absorption band appears at about 320 nm as a shoulder of the main UV transition.

Concerning the bromide salt, a CT band is also observed, but at higher energy compared to the iodide salt and only in

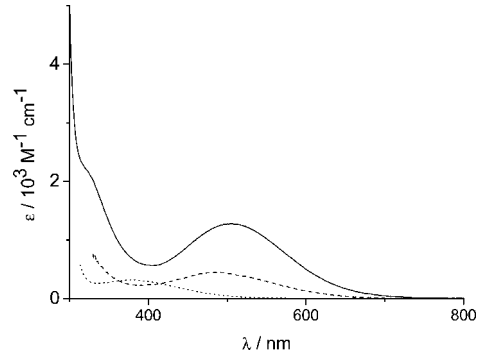

Figure 7. UV/vis spectra, of OVI_2 in (dot) methanol 3.4×10^{-3} M, (dash) acetone 1.1×10^{-4} M, and (solid) dichloromethane 1.4×10^{-4} M at 30 °C.

dichloromethane. No CT transition is detected in water and methanol, not even at the highest concentration investigated that is 0.022 M in methanol, although the shoulder of the UV absorption band, in the latter case, extends up to 400 nm. To summarize, in Table 4 we report the maximum absorption wavelengths, λ_{max}, for the various systems investigated.

TD-DFT Calculations. We deemed it of interest to investigate the absorption spectra of OVI_2 in dicholoromethane by TD-DFT calculations. Because of the softness of the charge distribution of the two moieties, the bipyridinium core and, even more, the iodide anion, and because of the strong attraction between the two, resulting in realtively short distances, see Table 1, a significant overlap of the electronic clouds should occur (see Figure S6 in Supporting Information). This circumstance renders the excited states of the ion-pair systems amenable to a semiquantitative treatment by TD-DFT methods, similarly to what reported in ref 19. This system offers another opportunity to test whether the prediction of TD-DFT for CT transitions in cases of large orbital overlap may be comparable with experimental results. If this turns out to be the case, the results of the calculations may help in understanding and assigning of the two additional bands, besides the $\pi-\pi^*$ bipyridinum transition, observed in dichloromethane.

First, it may be useful to compare the spectra calculated in solution phase using the gas-phase optimized geometries. This permits the separation of direct and indirect solvent effects, that is how the solvent directly affects the orbitals involved in the electronic transition and, on the other hand, how much of these changes is due to geometry differences. Previous calculations reported a dramatic solvent effect due to water.[22]

The calculated UV/vis spectra for model A are shown in Figure 8. The three highest occupied orbitals (see Figure S10 in Supporting Information) of the system are the 5 p orbitals of the iodide, while the lowest unoccupied orbitals are all localized on the bipyridinium core. Gas-phase TD-DFT calculation predict a weak absorption, not shown in the figure, corresponding to a HOMO−1 → LUMO transition, centered at 977 nm. Then we can observe a relatively strong absorption centered at 679 nm corresponding to the HOMO → LUMO transition and a second absorption above 300 nm corresponding to a HOMO−1 → LUMO+1 transition. The typical UV absorption band of the bipyridinium core is calculated at 280 nm and its main contribution comes from a HOMO−3 → LUMO transition, therefore it only involves the bipyridinium orbitals. In contrast, the two absorption bands observed in the visible region of the spectrum are both charge-transfer transitions.

The direct effect of the solvent is remarkable: even with a low-polar solvent as dichloromethane the weak transition at 977

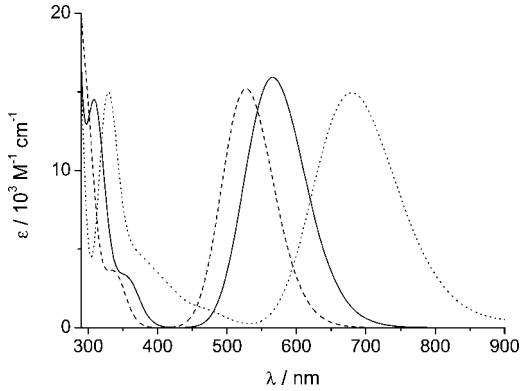

Figure 8. Simulated[36] UV/vis spectra of model A. TD-DFT calculation in (dot) gas phase, (solid) dichloromethane, and (dash) methanol.

nm disappears and the strong CT transition in the visible region is blue-shifted by more than 100 nm. Increasing further the dielectric constant produces an additional blue-shift, although less marked, in agreement with the experimental trend. Therefore TD-DFT calculations on the various model geometries considered have to be run including the solvent reaction field also for the case of low-polar solvents.

Thus, in Figure 9 we report the calculated vertical electronic transitions for the four model systems (A−D) together with the experimental spectrum in CH_2Cl_2. A detailed list of calculated parameters is reported in Supporting Information (Tables S1−S3).

It is noteworthy that all ion-pair models qualitatively agree in predicting a low energy transition (around 500−600 nm) essentially of HOMO → LUMO character and a high energy (around 300−350 nm) CT transition still to the LUMO orbital but originating from molecular orbitals mainly involving the remaining 5 p iodide orbitals not contributing to the HOMO. Clearly the $\pi-\pi^*$ bipyridinium transition is also very well predicted.

We may assume that all model ion-pairs contribute to the observed spectrum, although we do not have precise information of their population in solution (we note, however, that the most stable model geometry C gives a quantitative agreement). Thus in Figure 10 we compare the experimental spectrum with the simulated one[36] obtained using the averaged calculated parameters taking, for simplicity, the four model systems with the same weight. The agreement is rather good. We note that the intensity of the two CT bands compared with the intensity of the $\pi-\pi^*$ bipyridinium transition is calculated too high. However, the intensity depends on the exact position of the equilibria of eq 1, therefore a quantitative result cannot be obtained regarding this specific point.

Inspection of the monoelectronic orbital contributions to the various vertical transitions (see Tables S1 and S2 in Supporting Information) provides a consistent picture for the variuos models: the CT band observed at 506 nm (calcd 542 nm, which is an error of just 0.16 eV, incidentally this is very close to the mean absolute error of 0.14 eV reported for PBE0 TD-DFT calculations of covalent dyes[14]) is mainly due to a HOMO → LUMO excitation; however significant contributions of excitations to the LUMO orbital from the remaining p orbitals of iodide anion(s) are present. The HOMO and LUMO orbitals for model B are reported in Figure 11, as an example (the remaining can be found in Supporting Information, Figures S10 and S11). We note that, due to the close proximity of cation and anion, as already discussed, the HOMO is also delocalized on the bipyridinium core and, similarly, the LUMO is also in part delocalized on the iodide anion.

The CT band observed around 320 nm (calcd 309 nm) is mainly due to monoelectronic excitations from the lower p orbitals of iodide (these are HOMO−1 and HOMO−2 for the MVI^+ ion-pair models and HOMO−1 to HOMO−5 for MVI_2 ion-pair models) to higher virtual orbitals, LUMO+1, LUMO+2 and also LUMO+3. Finally the $\pi-\pi^*$ bipyridinium core transition is very little affected by ion-pairing: the experimental difference observed in water, methanol and dichloromethane is largely due to the direct solvent effect rather than to ion-pairing.[12] Calculations predict the bipyridinum core transition at 268 nm, that is almost coincident with the experimental value. The transitions contain only contributions of monoelectronic excitations from occupied orbitals lower than HOMO−2 and HOMO−5, for MVI^+ and MVI_2, respectively, that is not including the p orbitals of iodide.

How does this picture change if we consider geometries optimized using the PCM solvation scheme? As outlined above we have considered two different models optimized in solution. However, we note that optimizations using the solvent reaction field often failed to locate a well-defined minimum for the ion-pair. Since the electrostatic interaction is reduced, a rather flat potential energy surface is found concerning the position of the anion with respect to the cation. In fact, other minima have been found on the PES, which will not be discussed here.

Calculated vertical transitions for the model systems optimized in solution can be found in Table S3 of Supporting Information. Also in this case, two different CT bands are predicted with all three models, one in the visible region and the second one above 300 nm, together with the UV bipyridinium core transition. However, the calculated wavelength of the low energy CT band is significantly too high compared to the experimental value and the oscillator strength is largely reduced, by more than an order of magnitude compared to models A−D; these two results are consistent with the larger anion−cation distance and increased dihedral angle of the bipyridinium ring.

Conclusions

We have investigated the formation of ion-pairs of octyl viologen iodide in dichloromethane by means of NMR and UV/vis spectroscopy. The experimental results suggest that ion-pairs are formed which are responsible of the large deshielding of the *meta* protons of the bipyridinium ring and of the two intermolecular CT absorption bands between the iodide anion and the bipyridinium core. Comparison of calculated and experimental NMR data suggests that the distribution of the probability of finding an iodide anion around the dication has a large density also at the center of the bipyridinium core. Calculated UV/vis spectra are in good agreement with experiment using the same model geometries used for the NMR calculations. All the features of the experimental spectrum are reproduced including the relative position and intensity of the two bands belonging to the ion-pairs and having a CT character. Although the reliability of TD-DFT methods has often being questioned when dealing with CT transitions, thanks to the large orbital overlap between the two moieties, in this case, as in the few others reported in the literature, an insightful description of the excited electronic states can be achieved. Due to the widespread use of viologen salts in many areas of chemistry, from supramolecular to ionic liquids and liquid crystals science, we believe that assessing the viability of DFT approaches to study the effect of ion-pairing processes in low polar solvents on their spectroscopic properties represents an important contribution.

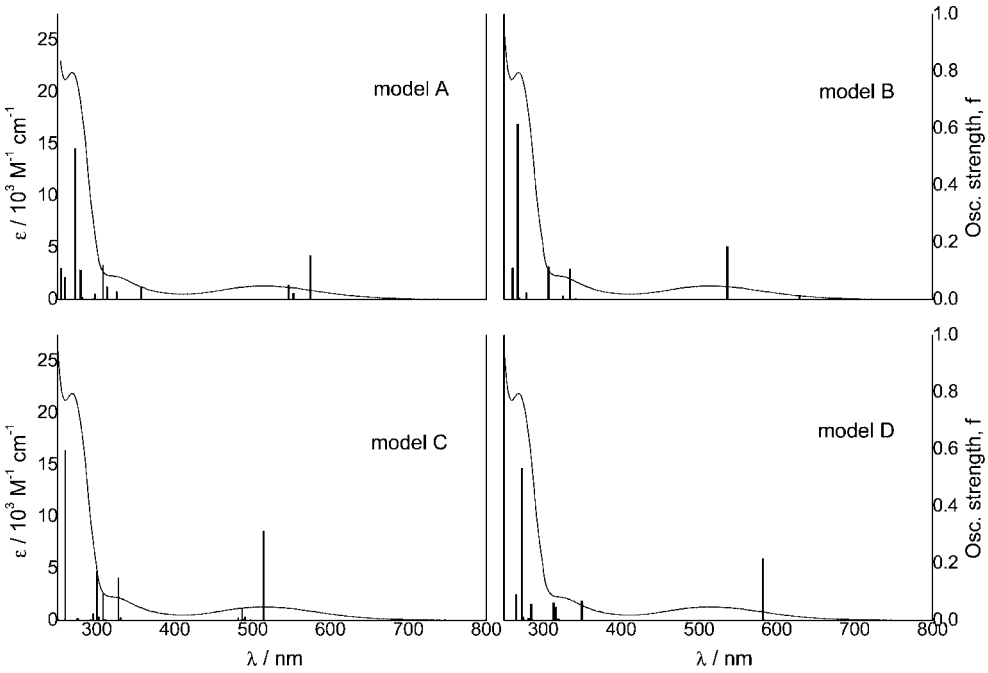

Figure 9. Experimental spectrum of octyl viologen diiodide in CH_2Cl_2 and calculated vertical electronic transitions of model ion-pairs A−D using the PCM solvation scheme (CH_2Cl_2) for the TD-DFT calculation.

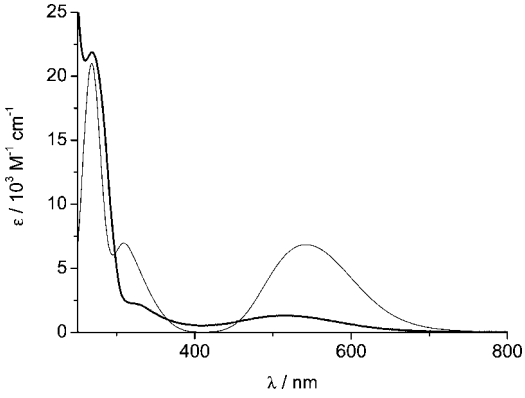

Figure 10. (thick line) Experimental and (thin line) simulated[36] spectrum of octyl viologen diiodide in CH_2Cl_2. The simulated spectrum is obtained using average calculated parameters from models A−D.

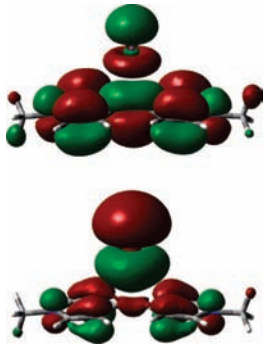

Figure 11. (bottom) HOMO and (top) LUMO molecular orbitals of the MVI^+ ion-pair, model B, PCM solvation scheme (CH_2Cl_2) for the single point calculation.

Supporting Information Available: NMR spectra of OVI_2, simulated UV/vis spectra, optimized geometries. This material is available free of charge via the Internet at http://pubs.acs.org.

Acknowledgment. All calculations were run on the Linux cluster at the Department of Chemistry (Laboratorio Interdipartimentale di Chimica Computazionale) of the University of Padova. Insightful comments of a reviewer are greatfully acknowledged.

References and Notes

(1) Monk, P. M. *The Viologens*; John Wiley & Sons: Chichester, U.K., 1998.

(2) (a) Moradpour, A.; Amouyel, E.; Keller, P.; Kagan, H. *Nouv. J. Chim.* **1978**, *2*, 547. (b) Keller, P.; Moradpour, A. *J. Am. Chem. Soc.* **1980**, *102*, 7193. (c) Launikonis, A.; Loder, J. W.; Mau, A.W.-H.; Sasse, W. H. F.; Wells, D. *Isr. J. Chem.* **1982**, *22*, 158. (d) Konigstein, C. *J. Photochem. Photobiol. A* **1995**, *90*, 141.

(3) Zen, J. M.; Lo, C. W. *Anal. Chem.* **1996**, *68*, 2635.

(4) Wang, J.; Wilcarius, A. *J. Electroanal. Chem.* **1996**, *107*, 183.

(5) Delacey, A. L.; Bes, M. T.; Gomezmoreno, C.; Fernandez, V. M. *J. Electroanal. Chem.* **1995**, *390*, 69.

(6) Byker, H. J. Gentex Corp. U.S. Patent 5,128,799, 1992.

(7) (a) Ballardini, R.; Balzani, V.; Credi, A.; Gandolfi, M. T.; Venturi, M. *Acc. Chem. Res.* **2001**, *34*, 445. (b) Credi, A.; Balzani, V.; Langford, S. J.; Stoddard, J. F. *J. Am. Chem. Soc.* **1997**, *119*, 2679.

(8) Yu, L.-P.; Samulski, E. T. In *Oriented Fluids and Liquid Crystals*; Griffin, A.C., Johnson, J. F., Eds.; Plenum: New York, 1984; Vol. 4, p 697.

(9) (a) Bhowmik, P. K.; Han, H.; Cebe, J. J.; Burchett, R. A.; Acharya, B.; Kumar, S. *Liq. Cryst.* **2003**, *30*, 1433. (b) Bhowmik, P. K.; Han, H.; Nedeltchev, I. K.; Cebe, J. J. *Mol. Cryst. Liq. Cryst.* **2004**, *419*, 27.

(10) (a) Arduini, A.; Calzavacca, F.; Pochini, A.; Secchi, A. *Chem. Eur. J.* **2003**, *9*, 793. (b) Credi, A.; Dumas, S.; Silvi, S.; Venturi, M.; Arduini, A.; Pochini, A.; Secchi, A. *J. Org. Chem.* **2004**, *69*, 5881.

(11) Huang, F.; Jones, J. W.; Selbodnik, C.; Gibson, H. W. *J. Am. Chem. Soc.* **2003**, *125*, 14458.

(12) di Matteo, A. *Chem. Phys. Lett.* **2007**, *439*, 190.

(13) (a) Koch, W.; Holthausen, M. C. *A Chemist Guide to Density Functional Theory*, 2nd ed.; Wiley-VCH: Weinheim, 2001. (b) Adamo, C.; Scuseria, G. E.; Barone, V. *J. Chem. Phys.* **1999**, *111*, 2889.

(14) Jacquemin, D.; Perpète, E. A.; Scuseria, G. E.; Ciofini, I.; Adamo, C. *J. Chem. Theory Comput.* **2008**, *4*, 123.

(15) (a) Miertus, S.; Scrocco, E.; Tomasi, J. *Chem. Phys.* **1981**, *55*, 117. (b) Cancès, M. T.; Mennucci, B.; Tomasi, J. *J. Chem. Phys.* **1997**, *107*, 3032. (c) Cossi, M.; Barone, V.; Mennucci, B.; Tomasi, J. *Chem. Phys. Lett.* **1998**, *286*, 253. (d) Mennucci, B.; Tomasi, J. *J. Chem. Phys.* **1997**, *106*, 5151. (e) Cossi, M.; Scalmani, G.; Rega, N.; Barone, V. *J. Chem. Phys.* **2002**, *117*, 43.

(16) (a) Dreuw, A.; Head-Gordon, M. *Chem. Rev.* **2005**, *105*, 4009. (b) Wanko, M.; Garavelli, M.; Bernardi, F.; Niehaus, T. A.; Frauenheim, T.; Elstner, M. *J. Chem. Phys.* **2004**, *120*, 1674. (c) Dreuw, A.; Weisman, J. L.; Head-Gordon, M. *J. Chem. Phys.* **2003**, *119*, 2943. (d) Dreuw, A.; Head-

Gordon, M. *J. Am. Chem. Soc.* **2004**, *126*, 4007. (e) Tozer, D. J.; Amos, R. D.; Handy, N. C.; Roos, B. O.; Serrano-Andres, L. *Mol. Phys.* **1999**, *97*, 859.

(17) Lange, A. W.; Rohrdanz, M. A.; Herbert, J. M. *J. Phys. Chem. B* **2008**, *112*, 6304.

(18) Improta, R. *Phys. Chem. Chem. Phys.* **2008**, *10*, 2656.

(19) Santoro, F.; Barone, V.; Improta, R. *J. Comput. Chem.* **2008**, *29*, 957.

(20) Santoro, F.; Barone, V.; Improta, R. *Proc. Natl. Ac. Sci. U.S.A.* **2007**, *104*, 9931.

(21) Bangal, P. R. *J. Phys. Chem. A* **2007**, *111*, 5536.

(22) Barone, V.; Fabrizi de Biani, F.; Ruiz, E.; Sieklucka, B. *J. Am. Chem. Soc.* **2001**, *123*, 10742.

(23) Bagno, A.; Rastrelli, F.; Saielli, G. *J. Org. Chem.* **2007**, *72*, 7373.

(24) Bagno, A.; D'Amico, F.; Saielli, G. *J. Phys. Chem. B* **2006**, *110*, 23004.

(25) (a) Stephens, P. J.; Devlin, F. J.; Chabalowski, C. F.; Frisch, M. J. *J. Phys. Chem.* **1994**, *98*, 11623. (b) Hertwig, R. H.; Koch, W. *Chem. Phys. Lett.* **1997**, *268*, 345.

(26) Packer, M. J.; Dalskov, E. K.; Enevoldsen, T.; Jensen, H. J. Aa.; Oddershede, J. *J. Chem. Phys.* **1996**, *105*, 5886.

(27) Dalton QM program "DALTON, a molecular electronic structure program, Release 2.0" (2005), see http://www.kjemi.uio.no/software/dalton/dalton.html.

(28) Dunning, T. H., Jr *J. Chem. Phys.* **1989**, *90*, 1007.

(29) Hehre, W. J.; Ditchfield, R.; Pople, J. A. *J. Chem. Phys.* **1972**, *56*, 2257.

(30) Glukhovstev, M. N.; Pross, A.; McGrath, M. P.; Radom, L. *J. Chem. Phys.* **1995**, *103*, 1878.

(31) Ciofini, I.; Adamo, C. *J. Phys. Chem. A* **2007**, *111*, 5549.

(32) Dunning, T. H., Jr.; Hay, P. J. In *Methods of Electronic Structure Theory*; Schaefer, H. F., III, Ed.; Plenum Press: New York, 1977; Vol. 2.

(33) (a) Bagno, A.; Saielli, G. *Theor. Chem. Acc.* **2007**, *117*, 603. (b) Bagno, A.; Rastrelli, F.; Saielli, G. *Chem. Eur. J.* **2006**, *12*, 5514.

(34) Frisch, M. J.; Trucks, G. W.; Schlegel, H. B.; Scuseria, G. E.; Robb, M. A.; Cheeseman, J. R.; Montgomery, J. A., Jr.; Vreven, T.; Kudin, K. N.; Burant, J. C.; Millam, J. M.; Iyengar, S. S.; Tomasi, J.; Barone, V.; Mennucci, B.; Cossi, M.; Scalmani, G.; Rega, N.; Petersson, G. A.; Nakatsuji, H.; Hada, M.; Ehara, M.; Toyota, K.; Fukuda, R.; Hasegawa, J.; Ishida, M.; Nakajima, T.; Honda, Y.; Kitao, O.; Nakai, H.; Klene, M.; Li, X.; Knox, J. E.; Hratchian, H. P.; Cross, J. B.; Bakken, V.; Adamo, C.; Jaramillo, J.; Gomperts, R.; Stratmann, R. E.; Yazyev, O.; Austin, A. J.; Cammi, R.; Pomelli, C.; Ochterski, J. W.; Ayala, P. Y.; Morokuma, K.; Voth, G. A.; Salvador, P.; Dannenberg, J. J.; Zakrzewski, V. G.; Dapprich, S.; Daniels, A. D.; Strain. M. C.; Farkas, O.; Malick, D. K.; Rabuck, A. D.; Raghavachari, K.; Foresman, J. B.; Ortiz, J. V.; Cui, Q.; Baboul, A. G.; Clifford, S.; Cioslowski, J.; Stefanov, B. B.; Liu, G.; Liashenko, A.; Piskorz, P.; Komaromi, I.; Martin, R. L.; Fox, D. J.; Keith, T.; Al-Laham, M. A.; Peng, C. Y.; Nanayakkara, A.; Challacombe, M.; Gill, P. M. W.; Johnson, B.; Chen, W.; Wong, M. W.; Gonzalez, C.; Pople, J. A. *Gaussian 03*, Revision C.02, Gaussian Inc.: Wallingford, CT, 2004.

(35) Schuchardt, K. L.; Didier, B. T.; Elsethagen, T.; Sun, L.; Gurumoorthi, V.; Chase, J.; Li, J.; Windus, T. L. Basis Set Exchange: A Community Database for Computational Sciences. *J. Chem. Inf. Model.* **2007**, *47*, 1045.

(36) Gorelsky, S. I. SWizard program, http://www.sg-chem.net/, CCRI, University Of Ottawa, Ottawa, Canada, 2008.

(37) Gottlieb, H. E.; Kotlyar, V.; Nudelman, A. *J. Org. Chem.* **1997**, *62*, 7512.

(38) Russell, J. H.; Wallwork, S. C. *Acta Crystallogr. B* **1972**, *28*, 1527.

(39) Eckert, N. A.; Krause Bauer, J. A.; Connick, W. B. *Acta Crystallogr.* **1994**, *C55*, IUC9900101.

(40) A very noisy ^{1}H spectrum was obtained after 1000 scans for a saturated solution in chloroform while no ^{1}H signal was observed after 1000 scans for a saturated benzene solution.

(41) (a) Wodrich, M. D.; Corminboeuf, C.; Schleyer, P. v. R. *Org. Lett.* **2006**, *8*, 3631. (b) Schreiner, P. R.; Fokin, A. A.; Pascal, R. A.; deMeijere, A. *Org. Lett.* **2006**, *8*, 3635.

(42) Bagno, A.; Butts, C.; Chiappe, C.; D'Amico, F.; Lord, J. C. D.; Pieraccini, D.; Rastrelli, F. *Org. Biomol. Chem.* **2005**, *3*, 1624.

(43) Bagno, A.; Rastrelli, F.; Saielli, G. *Prog. NMR Spectrosc.* **2005**, *47*, 41.

(44) Rose, N. J.; Drago, R. S. *J. Am. Chem. Soc.* **1959**, *81*, 6138.

(45) Nordio, P. L.; Polimeno, A.; Saielli, G. *J. Photochem. Photobiol. A: Chem.* **1997**, *105*, 269.

(46) Watanabe, T.; Honda, K. *J. Phys. Chem.* **1982**, *86*, 2617.

(47) Monk, P. M. S.; Hodgkinson, N. M.; Partridge, R. D. *Dyes Pigm.* **1999**, *43*, 241.

(48) (a) Chandramouleeswaran, S.; Vijaylakshmi, B.; Kartihkeyan, S.; Rao, T. P.; Iyer, C. S. P. *Mikrochim. Acta* **1998**, *128*, 75. (b) Bradforth, S. E.; Jungwirth, P. *J. Phys. Chem. A* **2002**, *106*, 1286.

JP802747H